JBC Papers in Press. Published on September 19, 2019 as Manuscript RA118.006961
The latest version is at http://www.jbc.org/cgi/doi/10.1074/jbc.RA118.006961

Epidermal growth factor (EGF) triggers nuclear calcium signaling through the intranuclear phospholipase C delta-4 (PLCδ4)

Marcelo Coutinho de Miranda[1,6#], Michele Angela Rodrigues[1,6#], Ana Carolina de Angelis Campos[1,6#], Jerusa Araújo Quintão Arantes Faria[2#], Marianna Kunrath-Lima[1], Gregory A. Mignery[3], Deborah Schechtman[4], Alfredo Miranda Goes[5], Michael H. Nathanson[6], and Dawidson A. Gomes[1,6*]

From the [1]Department of Biochemistry and Immunology, Universidade Federal de Minas Gerais (UFMG), Av. Antonio Carlos, 6627, Belo Horizonte – MG, 31270-901, Brazil; [2]Department of Physiology Sciences, Universidade Federal do Amazonas, Manaus - AM, Brazil; [3]Department of Cell and Molecular Physiology, Stritch School of Medicine, Loyola University Chicago, Maywood – IL, 60153, USA; [4]Department of Biochemistry, University of São Paulo. Av. Professor Lineu Prestes, 748, São Paulo – SP, 05508-900, Brazil; [5]Department of Pathology, UFMG; [6]Section of Digestive Diseases, Internal Medicine, Yale University. 333 Cedar St, New Haven – CT, 06520-8056, USA.

Running title**:** PLCδ4 mediates EGF-induced Ca^{2+} signals and cell proliferation

[#]Contributed equally

*To whom correspondence should be addressed: Dawidson A. Gomes. E-mail: dawidson@icb.ufmg.br; *Instituto de Ciências Biológicas, bloco Q4, sala 238. Universidade Federal de Minas Gerais. Av. Antônio Carlos, 6627. Belo Horizonte – MG,* Zip Code: *31270-901, Brazil.*

Keywords: epidermal growth factor receptor (EGFR), phosphatidylinositol 4,5-bisphosphate ($PI(4,5)P_2$), nucleus, calcium, protein kinase C (PKC), phospholipase Cδ-4 (PLCδ4), proliferation, receptor tyrosine kinases (RTKs), cell signaling.

ABSTRACT

Calcium (Ca^{2+}) signaling within the cell nucleus regulates specific cellular events such as gene transcription and cell proliferation. Nuclear and cytosolic Ca^{2+} levels can be independently regulated, and nuclear translocation of receptor tyrosine kinases (RTKs) is one way to locally activate signaling cascades within the nucleus. Nuclear RTKs, including the epidermal growth factor receptor (EGFR), are important for processes such as transcriptional regulation, DNA-damage repair, and cancer therapy resistance. RTKs can hydrolyze phosphatidylinositol 4,5-bisphosphate ($PI(4,5)P_2$) within the nucleus, leading to Ca^{2+} release from the nucleoplasmic reticulum (NR) by inositol 1,4,5-trisphosphate receptors ($InsP_3R$). $PI(4,5)P_2$ hydrolysis is mediated by phospholipase C (PLC). However, it is unknown which nuclear PLC isoform is triggered by EGFR. Here, using subcellular fractionation, immunoblotting and fluorescence, siRNA-based gene knockdowns, and FRET-based biosensor reporter assays, we investigated the role of PLCδ4 in EGF-induced nuclear Ca^{2+} signaling and downstream events. We found that EGF-induced Ca^{2+} signals are inhibited when translocation of EGFR is impaired. Nuclear Ca^{2+} signals also were reduced by selectively buffering inositol 1,4,5-trisphosphate ($InsP_3$) within the nucleus. EGF induced hydrolysis of nuclear $PI(4,5)P_2$ by the intranuclear PLCδ4, rather than by PLCγ1. Moreover, protein kinase C (PKC), a downstream target of EGF, was active in the

nucleus of stimulated cells. Furthermore, PLCδ4 and $InsP_3$ modulated cell cycle progression by regulating the expression of cyclins A and B1. These results provide evidence that EGF-induced nuclear signaling is mediated by nuclear PLCδ4, and suggest new therapeutic targets to modulate the proliferative effects of this growth factor.

Introduction

The spatial-temporal distribution of calcium (Ca^{2+}) signals contributes to the versatility of this second messenger (1). For example, increases in Ca^{2+} within the cell nucleus selectively promote cellular events such as gene transcription (2), cell proliferation and tumor growth (3). Moreover, nuclear Ca^{2+} signals can be regulated independently of cytosolic Ca^{2+} signals (4). This is possible because the nucleus contains the machinery necessary for Ca^{2+} mobilization (5–8). Specifically, the nuclear envelope (NE) is contiguous with the endoplasmic reticulum (ER) (9) and has invaginations that can reach deep within the nucleoplasm (10). These invaginations express $InsP_3Rs$ and store and release Ca^{2+} in an $InsP_3$-sensitive fashion (5, 11), and have been referred to as the nucleoplasmic reticulum (NR) (5, 10). The distribution of $InsP_3R$ isoforms and also Ca^{2+} signaling in the nucleus become altered in various disease states, such as fatty liver disease (12) and cholangiocarcinoma (13). Intranuclear $InsP_3$ is formed from $PI(4,5)P_2$ hydrolysis, which is induced by growth factors such as hepatocyte growth factor (7) and insulin (8). Some RTKs undergo nuclear translocation upon activation, which appears necessary for initiation of nuclear Ca^{2+} signals (7, 8), so this could be one mechanism to regulate Ca^{2+} release locally.

Nuclear localization of EGFR is of clinical relevance, as it is correlated with cancer prognosis (14) and relates to resistance to various cancer therapies (15, 16). Nuclear EGFR function has been the subject of extensive investigation, as has been nuclear targets of EGFR. EGFR can shuttle from the cell surface to the nucleus (17, 18) where it acts as a transcriptional regulator (19, 20), transmits signals (21, 22), and is involved in processes such as cell proliferation, tumor progression, and DNA repair and replication (23). However, it is unknown if EGFR is linked to nuclear calcium release.

PLC could be involved in primary nuclear Ca^{2+} signaling since activation of $InsP_3$ receptors generally is involved in the release of Ca^{2+} in the nucleus (24). In mammals, the PLC family is composed of 13 isozymes, divided into 6 classes: β, γ, δ, ε, ζ and η, according to their structures (25). All these isozymes catalyze the reaction of $PI(4,5)P_2$ cleavage, generating $InsP_3$ and diacylglycerol (DAG), but each one possesses unique physiological functions (25). Some PLCs are described within the nucleus in specific cell types such as PLCβ1, PLCγ1, PLCδ1, PLCδ4 and PLCζ (26, 27). The activity of these nuclear PLCs is related to the regulation of several cellular processes, such as proliferation and differentiation. These particular isoforms also have been linked to specific diseases, including myelodysplastic syndromes (PLCβ1), neurological diseases (PLCγ1) and infertility (PLCζ and PLCδ1-4) (28).

PLCδ4 has been identified as a nuclear protein in different cell types and may be involved in proliferative processes (27, 29–31). It was first purified from regenerating rat liver protein extracts (32), and its gene was cloned (33) from a regenerating rat liver cDNA library, indicating a possible role of PLCδ4 in cell proliferation. Despite its nuclear localization, it is unknown how human PLCδ4 is activated within the nucleus. This work investigates whether EGFR activates nuclear Ca^{2+} signaling via PLCδ4.

Results

EGFR translocates to the nucleus and induces Ca^{2+} signals

Stimulation with EGF induces its RTK EGFR to translocate to the nucleus (18), similar to what has been shown for other RTKs, including the hepatocyte growth factor (HGF) receptor, c-Met, and the insulin receptor (7, 8). EGFR translocated to the nucleus in both primary rat hepatocytes and SKHep-1 cells, a human liver cancer cell line (Fig. 1A). EGFR protein levels in the nuclear fraction were higher than in non-stimulated control cells as soon as 2.5 min after stimulation with EGF (Fig. 1A). In SKHep-1 cells, EGFR decreased in the non-nuclear fraction as it increased in the nuclear fraction. The peak of EGFR nuclear translocation in this cell line was at

10 min (Fig. 1A). Super-resolution immunofluorescence showed that EGFR accumulated in the nucleus within 10 min of exposure to EGF (Fig. 1B). EGF stimulation induced bigger EGFR clusters throughout the cells, including at the nucleus, as previously demonstrated (15). These data demonstrate that EGF induces EGFR to translocate to the nucleus.

Translocation of EGFR to the nucleus depends on Clathrin-mediated endocytosis (17), so we used Clathrin heavy chain 2 (CHC2) siRNAs to disrupt this endocytic pathway and thereby inhibit internalization of EGFR. Figure 1C shows that siRNA treatment reduced CHC2 expression by 94 ± 3% using the CHC2 siRNA 1 and by 87 ± 8% using the CHC2 siRNA 2, relative to control ($p<0.001$). Stimulation of control cells with EGF led to a gradual Ca^{2+} increase with some superimposed oscillations, similar to the Ca^{2+} signal pattern induced by other growth factors (7, 8), but CHC2 knockdown diminished the peak of EGF-induced Ca^{2+} signals by 85 ± 2% ($p<0.001$) using the CHCH2 siRNA 1 and by 100 ± 2% ($p<0.001$) using the CHCH2 siRNA 2, compared to control (Fig. 1D). This indicates that most of the Ca^{2+} signals induced by EGF depend on EGFR internalization.

EGF triggers intranuclear PI(4,5)P_2 hydrolysis and InsP_3 formation

EGF induces intracellular Ca^{2+} transients through $InsP_3$ (34), so we investigated whether EGF-induced $InsP_3$ formation in the nucleus was responsible for increasing intranuclear Ca^{2+}. SKHep-1 cells were transfected with cytosolic or nuclear $InsP_3$-buffer constructs whose targeting was confirmed by subcellular localization of the monomeric red fluorescent protein (mRFP) (Fig. 2A). Fluo-4/AM was used to monitor Ca^{2+} release in response to EGF. Cytosolic $InsP_3$-buffer decreased the Ca^{2+} response by 50.5 ± 6.1% in the nucleus and by 53.8 ± 4.5% in the cytoplasm (Fig. 2B), but EGF-induced Ca^{2+} signals were decreased by 86 ± 2.7% in the nucleus and by 96 ± 3.9% in the cytoplasm in cells expressing the nuclear $InsP_3$-buffer (Fig. 2B). This suggests that EGF triggers nuclear Ca^{2+} signals by inducing the formation of $InsP_3$ within the nucleus, similar to what has been observed in liver cells stimulated with HGF (7) or insulin (8). To investigate whether EGF induces nuclear PI(4,5)P_2 hydrolysis to produce $InsP_3$, PI(4,5)P_2 was measured in nuclear fractions of hepatocytes. Nuclei from EGF-stimulated cells contained 64 ± 1.5% less PI(4,5)P_2 than nuclei from control cells (Fig. 2D). These findings provide evidence that EGF triggers nuclear PI(4,5)P_2 hydrolysis and local $InsP_3$ production to generate Ca^{2+} signals.

EGF stimulates intra-nuclear PKC activity

PI(4,5)P_2 hydrolysis generates not only $InsP_3$ but also DAG, which can activate PKC (24). Increases in nuclear DAG can either participate in translocation of PKCs, from the cytosol to the nucleus, or can directly activate PKCs that reside in the nucleus (35). To determine whether EGF triggers nuclear PKC activity, we used a Förster resonance energy transfer (FRET) reporter based on PKC activity and tagged to a nuclear localization signal (NucCKAR) (36). The nuclear localization of this construct was confirmed by intra-nuclear detection of cyan fluorescent protein (CFP) and yellow fluorescent protein (YFP) fluorescence by confocal microscopy (Fig. 3A). Phosphorylation of the reporter by PKC results in decreased rather than increased FRET (36), so CFP/YFP ratio was monitored to reflect PKC activity. NucCKAR-expressing SKHep-1 cells were stimulated with EGF, phorbol 12-13-dibutyrate (PdBu) as a positive control for PKC activation, or arginine vasopressin (AVP) to reflect cytosolic activation of PKC, and then changes in FRET were followed for 30 min (Fig. 3B). PdBu increased CFP/YFP emission of NucCKAR (Fig. 3B and 3C) and similar results were obtained with EGF treatment (Fig. 3B and 3C), indicating that either stimulus increases nuclear PKC activity. Unlike EGF, stimulation with AVP, which activates a prototypical G protein-coupled receptor in the plasma membrane, did not increase the CFP/YFP emission ratio of NucCKAR (Fig. 3B and 3C). This result suggests that subplasmalemmal formation of DAG in response to AVP does not activate nuclear PKC. Treatment with the broad-range PKC inhibitor Go6983 (Fig. 3D) decreased EGF-induced CFP/YFP emission ratio, providing additional evidence that EGF triggers PKC activity within the nucleus.

PLCγ1 is localized to the cytosol and PLCδ4 is in the nucleus

PLC mediates $PI(4,5)P_2$ hydrolysis (28) and formation of $InsP_3$ and DAG (29, 30), so the relative role played by several candidate PLC isoforms during EGF stimulation was investigated. PLCγ1 is the primary isoform typically thought to bind to and be activated by RTKs (1). PLCδ4 has been recognized as a predominantly nuclear PLC isoform, and its expression is increased in liver regeneration (33), so we compared the localization of these two isoforms in SKHep-1 cells. Confocal immunofluorescence showed that PLCγ1 is mostly localized to the cytosol, and this pattern does not change upon EGF stimulation (Fig. 4A). In contrast, PLCδ4 was detected exclusively in the nucleus of SKHep-1 cells, demonstrated by both confocal microscopy (Fig. 4B) and western blot (not shown). The subcellular localization of these PLC isoforms was also assessed in primary rat hepatocytes. Similar to what was observed in SKHep-1 cells, PLCγ1 was found in non-nuclear fractions of both control and EGF-stimulated cells, whereas PLCδ4 was only detected in the nuclear fractions (Fig. 4C). The amount of PLCγ1 or PLCδ4 in each cell fraction was not altered by stimulation with EGF (Fig. 4C), indicating that there is no translocation of these PLCs between nuclear and non-nuclear compartments in response to EGF. Further examination showed that EGF stimulation for up to 10 min does not induce PLCγ1 to translocate from the cytoplasm to the nucleus (Fig. 4D).

PLCδ4 participates in EGF-induced nuclear $PI(4,5)P_2$ hydrolysis, $InsP_3$ signaling, Ca^{2+} signals and PKC activity

A siRNA approach was employed to determine the relative roles of PLCδ4 and PLCγ1 in EGF-induced nuclear $PI(4,5)P_2$ hydrolysis and Ca^{2+} signaling. Specific siRNAs reduced PLCγ1 expression by 90 ± 14% and 91 ± 27% using siRNA 1 and 2, respectively. PLCδ4 expressions were reduced by 75 ± 7% and 86 ± 5% using siRNA 1 and 2, respectively ($p<0.01$) (Fig. 5A). Nuclear fractions were isolated from these cells after EGF stimulation and $PI(4,5)P_2$ was quantified. EGF significantly increased nuclear $PI(4,5)P_2$ hydrolysis in control siRNAs and PLCγ1 siRNA-treated cells, but not in PLCδ4 siRNA-treated cells (Fig. 5B). Furthermore, cells treated with PLCδ4 siRNAs significantly reduced nuclear $InsP_3$ production, nuclear PKC activity and Ca^{2+} signals, but this was not seen in PLCγ1 siRNA-treated cells (Fig. 5C-E). These results suggest that PLCδ4 but not PLCγ1 participates in nuclear $PI(4,5)P_2$ hydrolysis, $InsP_3$ production, PKC activation and Ca^{2+} signaling triggered by EGF stimulation.

PLCδ4 participates in cell cycle progression

Nuclear Ca^{2+} is important for cell proliferation (3), an important downstream effect of EGF. Therefore, we investigated whether PLCδ4 is involved in EGFR-mediated cell proliferation. Cell proliferation as measured by either cell counting (Fig. S1) or BrdU incorporation (Fig. 6A) was decreased by over 67% in cells in which PLCδ4 expression was reduced. SKHep-1 proliferation was restored when PLCδ4 expression was recovered (Fig. S1). Cell death does not mediate the decreased proliferation since Annexin V-FITC, and propidium iodide assays did not reveal cell death between control and siRNA treated groups (Fig. 6B). Next, the role of PLCδ4 in cell cycle progression was investigated. To understand the basis for this, the effects of PLCδ4 on the expression of various cyclins was studied (Fig. S1). Expression of cyclin B1, a G2/M-phase checkpoint protein, and cyclin A, an S-phase checkpoint protein, were decreased in PLCδ4 knockdown cells compared to cells treated with control siRNA (Fig. 6C). A nuclear $InsP_3$-buffer also decreased the expression of cyclins A and B. These findings suggest that nuclear PLCδ4 affects cell cycle progression, in part by affecting cyclin expression.

Discussion

EGFR has several direct effects on signaling in the nucleus, including interaction with transcription factors (37) and phosphorylation (21). The current work extends this repertoire of intranuclear actions by showing that EGFR translocates to the nucleus of hepatic cells to initiate $InsP_3$-mediated Ca^{2+} signals. EGFR likely

translocates from the plasma membrane to the nucleus via the ER (20, 23), and a similar trafficking route has been described for both viruses and toxins as well (38–40). Trafficking of other RTKs from the plasma membrane to the nucleus has also been described. For example, c-Met that is biotinylated at the plasma membrane can be recovered from the nucleus after cells are stimulated with HGF (7). Similarly, fluorescently labeled EGF can be tracked from the cell membrane to the cell nucleus over a 10-minute period (18). Furthermore, super-resolution imaging can be used to quantify the amount of EGF/EGFR clusters that accumulate in the nucleus (18). The peak in nuclear translocation of EGFR coincides with the peak in Ca^{2+} signals (Fig. 1A-C). The current work builds on the previous observation that translocation of EGFR to the nucleus depends on dynamin and clathrin-mediated endocytosis (17) by showing that knockdown of clathrin reduces EGF-induced Ca^{2+} signals. These findings are consistent with the idea that EGFR must translocate to the nucleus in order to initiate nuclear Ca^{2+} signals, similar to what has been shown for c-Met (7).

Ca^{2+} signaling in the nucleus rather than cytosol is important for proliferation and tumor growth (3). Nuclear Ca^{2+} also can regulate gene expression (2, 4). Thus, increases in nuclear Ca^{2+} could be one mechanism for EGF to promote those cellular processes. The nucleus contains the machinery necessary for $InsP_3$ receptor-mediated Ca^{2+} release (5, 7, 8, 24). Although PLC-mediated $PI(4,5)P_2$ hydrolysis and formation of $InsP_3$ and DAG within the cytoplasm has been described extensively (1), there are fewer studies showing that $PI(4,5)P_2$ hydrolysis also occurs within the nucleus. The current work provides evidence that EGF triggers $PI(4,5)P_2$ hydrolysis and $InsP_3$ formation within the nucleus (Fig. 2 and 5), similar to what has been observed in response to stimulation with HGF (7) or insulin (8).

PLC within the nucleus is involved in signal transduction pathways that are separate from those activated by isoforms localized in other compartments (41). The most common paradigm links PLC beta isoforms with G protein-coupled receptors, whereas RTKs typically are associated with PLC gamma isoforms (42). For example, activated nuclear metabotropic glutamate 5 (mGlu5) receptor couples to $G_{q/11}$ and a nuclear isoform, PLCβ1 to generate the $InsP_3$-mediated release of Ca^{2+} from Ca^{2+}-release channels in the nucleus of primary striatal neurons (43). The current work provides evidence that EGF induces hydrolysis of nuclear $PI(4,5)P_2$ by the intra-nuclear PLCδ4, rather than by PLCγ1 (Fig. 5). It remains unclear whether PLCδ4 is activated directly or indirectly, as a direct binding of PLCδ4 with nuclear EGFR could not be demonstrated by co-immunoprecipitation (not shown).

There are a number of previous studies about the function of nuclear PLCs. Some studies suggest that PLC positively regulates the cell cycle. PLCβ1 can regulate IGF (insulin-like growth factor)-1-stimulated DNA synthesis and its overexpression increases proliferation in the absence of mitogenic stimuli (44, 45). Furthermore, PLCβ1 in the nucleus regulates transcriptional levels of genes such as cyclin D3 and c-jun activation in skeletal muscle cells (45, 46). The present study demonstrates that PLCδ4 also plays a role in cellular proliferation and specifically in cell-cycle control. Knockdown of PLCδ4 leads to decreased cell proliferation without affecting apoptosis in SKHep-1 cells (Fig. 6). The cell cycle profile is accompanied by reduced expression of cyclins A and B1 (Fig. 6). Consistent with this, decreased cyclin B1 could interfere with the transition through the G2/M phase of the cell cycle. Furthermore, it was demonstrated that PLCδ4 knockdown impaired human mesenchymal stem/stromal cells proliferation, without inducing cell death (31).

The direct target of PLC signaling is typically PKC, which is activated by the $PI(4,5)P_2$ hydrolysis products DAG and $InsP_3$ (35). Because EGF activates PKC within the nucleus (Fig. 3), and several nuclear proteins are PKC substrates, this may also be relevant for processes such as gene expression and changes in chromatin structure (47). Activation of PKC may affect cell cycle progression as well (48, 49). PKCα is necessary for PLCβ1 mediated regulation of cyclin D3 and cell proliferation in human erythroleukemia cells (50), and PKCα regulates cyclin B1 leading to effects on G2/M transition. PKC inhibitors can decrease cyclin B1 expression consequent to PKCs down-regulation (51). The increase in nuclear DAG level observed during the G2 phase is sufficient to activate nuclear PKCα/PKCβ. PKC phosphorylates Lamin B1 at

sites involved in mitotic disassembly of the nuclear lamina, one of the most critical events in the G2/M transition (52).

In light of these consideration, the current findings identify novel signaling events that may link EGFR nuclear translocation to stimulation of cell growth (Fig. 7). Activation of this signaling pathway may, in turn, be important for hepatocytes proliferation, especially because liver regeneration is absolutely dependent on the presence of either EGF or HGF (53). This also is consistent with the observation that PLCδ4 expression is increased in liver regeneration as well as in liver cancer cell lines (54, 55). It furthermore is consistent with data from PLCδ4 knockout mice that show increases in Bromodeoxyuridine (BrdU) are delayed after partial hepatectomy, although liver regeneration is not delayed (55). Therefore, strategies to selectively inhibit PLCδ4 could be important for selective inhibition of liver cancer, which is the third leading cause of cancer death worldwide.

Experimental procedures

Cell culture and EGF stimulus

The SKHep-1 is a human liver cancer cell line (ATCC, VA, USA). It was cultured at 37°C in 5% CO_2 in Dulbecco's modified Eagle's medium (Life Technologies, CA, USA) containing 10% fetal bovine serum, 1 mM sodium pyruvate, 100 units/ml penicillin, and 100 µg/ml streptomycin (Life Technologies).

Hepatocytes were isolated from healthy male Sprague Dawley rats (190-200g; Charles River Laboratories, MA, USA), as described previously (56). Primary cells were cultured at 37°C in 5% CO_2 in Williams' medium E (Life Technologies) containing 10% fetal bovine serum, 100 units/mL penicillin, and 100 µg/mL streptomycin and plated on collagen-coated coverslips (50 µg/mL) (BD Biosciences, CA, USA). Hepatocytes were used within 24 hours of isolation. All animal studies were approved by the Yale University Institutional Animal Care and Use Committee under Protocol # 2018-07602.

Serum-starved (14-16 hours) cells were treated with 100 ng/mL of human recombinant EGF (Life Technologies) or recombinant rat EGF (R&D Systems, MN, USA) at 37°C in 5% CO_2.

Subcellular fractionation and western blot

Cells were washed twice with ice-cold 10 mM phosphate-buffered saline pH 7,4 (PBS) (Sigma-Aldrich, CA, USA), harvested by scraping, and lysed in a buffer with 20 mM 4-(2-hydroxyethyl)-1-piperazine ethanesulfonic acid, pH 7.0, 10 mM KCl, 2 mM $MgCl_2$, 0.5% Nonidet P-40. After incubation on ice for 10 min, the cells were homogenized by vortex. The homogenate was centrifuged at 1,500*g* for 5 min to sediment the nuclei. The supernatant was then centrifuged at a maximum speed of 16,100*g* for 20 min, and the resulting supernatant formed the non-nuclear fraction. The nuclear pellet was washed three times with lysis buffer to remove any contamination from cytoplasmic membranes. The isolated nuclei were resuspended in NETN buffer (150 mM NaCl, 1 mM EDTA, 20 mM Tris-HCl, pH 8.0, 0.5% Nonidet P-40), and the mixture was sonicated briefly to aid nuclear lysis. Nuclear lysates were collected after centrifugation at 16,100*g* for 20 min at 4°C. Protease and phosphatase inhibitors (Sigma-Aldrich) were added to all buffers. Proteins were quantified by Bradford assay (Sigma-Aldrich).

Western blotting was performed and detected as described previously (7). In Brief, primary antibodies used were: rabbit polyclonal anti-EGFR (1:500, Santa Cruz Biotechnology, TX, USA, cat. SC3), mouse monoclonal anti-EGFR clone 8G6.2 (1:500, Millipore/Sigma-aldrich, cat. 05-1047), mouse monoclonal anti-α-Tubulin (1:2000, Sigma-Aldrich, cat. T6199), rabbit polyclonal anti-Lamin B1 (1:2000, Abcam, MA, USA, cat. ab16048), monoclonal anti-Clathrin (1:500, Abcam, cat. b21679), mouse monoclonal anti-PLCγ1 (1:1000, Cell Signaling Technology, MA, USA, cat. I2822) and rabbit polyclonal anti-PLCδ4 (1:500, Santa Cruz Biotechnology, cat. H-250), rabbit polyclonal Erk1/2 (1:1000; Cell Signaling, cat. 9101), rabbit monoclonal anti-phospho-Erk1/2 T202/Y204 (1:1000; Cell Signaling, cat. 4370), rabbit monoclonal anti-AKT (1:1000, Cell Signaling, cat. 4691), rabbit monoclonal anti-phospho-AKT T308 (1:1000; Cell Signaling, cat. 13038), cyclins A, B1, D1, D2, D3, E, E2 and H (1:500 to 1000, Cell Signaling Technology, Kit cat. 9869). The membranes were developed using ECL Plus (GE Healthcare Life Sciences, Piscataway, NJ, USA). Subsequently, the films were scanned and

analyzed using Image J software (http://rsbweb.nih.gov/ij/). All antibodies used were found to have the correct molecular weight by western blot. The antibodies for Clathrin, PLCδ4 and PLCγ1 were validated with at least two specific siRNAs.

Immunofluorescence

Confocal and super-resolution immunofluorescence imaging were performed as described previously (18). In brief, cells were labeled with rabbit polyclonal anti-EGFR (1:250, Santa Cruz Biotechnology, cat. SC3) or mouse monoclonal anti-EGFR clone 8G6.2 (1:200, Millipore/Sigma-Aldrich, cat. 05-1047), rabbit polyclonal anti-PLCγ1 (1:200, Cell Signaling, I2822) and polyclonal anti-PLCδ4 (Santa Cruz Biotechnology, cat. H-250) and then incubated with secondary antibodies conjugated to Alexa Fluor 488 or 546 (Life Technologies). Hoechst 33342 (Life Technologies) was used as a marker for the nuclear compartment. Images were collected using a Leica SP8 Gated STED super-resolution microscope with a 100X, 1.4 NA objective lens.

siRNA transfection

Cells were transfected using Lipofectamine RNAiMAX reagent (Life Technologies) according to the manufacturer's instructions. 50 nM siRNAs were used for Clathrin Heavy Chain knockdown (CHC2 siRNA 1, 5`-GCAAUUAAUUAAGGCUGACCGUAtt-3`, Life Technologies, cat. s223263; CHC2 siRNA 2, 5`-AGGUGGCUUCUAAAUAUCAUGAACA-3`, IDT, cat. hs.Ri.CLTC.13.1). 25 nM siRNAs were used for PLCγ1 knockdown (PLCγ1 siRNA 1, 5`-GAAUCGUGAGGAUCGUAUAtt-3`, Life Technologies, cat. s10632; and PLCγ1 siRNA 2, 5`-GACCUCAUCAGCUACUAUGAGAAAC-3`, IDT, cat. hs.Ri.PLCG1.13.1). For PLCδ4 knockdown 50 nM of the following siRNAs were used: ON-TARGETplus SMARTpool (PLCδ4 siRNA 1, 5`-CAAGAAGUUCAGCGGUUAU-3`, 5`-GCUCAAUCCCAUACCGACA-3`, 5`-GACCAAUGGCUGAGCGAUU-3`, CAACAAGGUUACCGCCACA Dharmacon, CO, USA, cat. L-005065-01) and PLCδ4 siRNA 2 (5`-AAGGCAGGUUGCAACUAGAAAUUCA-3`, IDT, cat. hs.Ri.PLCD4.13.3,). 50 nM of the following non-targeting siRNAs were used: Silencer™ Select Negative Control No. 2 siRNA (control siRNA 1, Life Technologies, cat. 4390846,) and IDT Scrambled negative control DsiRNA (control siRNA 2, 5`-CUUCCUCUCUUUCUCUCCCUUGUGA-3`, cat. 51-01-19-08). Further analysis was performed 48 hours after transfection.

$InsP_3$-buffer constructs and calcium imaging

Generation of $InsP_3$-buffer constructs was as described previously (7). Briefly, the $InsP_3$ binding domain (residues 224-605) of the human type I $InsP_3$ receptor was tagged with a mRFP and with a nuclear localization signal or nuclear exclusion signal to generate the nuclear and cytosolic constructs, respectively. The adenovirus were built by ViraQuest Inc. Cells were infected with 10 MOIs and analysis performed in 48 hours. For calcium imaging cells were incubated with 5 μM Fluo-4/AM (Life Technologies) and placed in a custom-made perfusion chamber for EGF stimulation. Images were collected with a Zeiss LSM 710 DUO NLO. Nuclear and cytosolic regions were selected with the assistance of the brightfield images.

Nuclear $PI(4,5)P_2$ extraction and detection

$PI(4,5)P_2$ from samples was detected by a mass ELISA assay kit (Echelon Biosciences, UT, USA). Upon 5 min EGF stimulation cell nuclei were isolated as previously described (7, 8), washed three times with PBS and followed with $PI(4,5)P_2$ extraction as recommended by the kit manufacturer. In summary, the protein was precipitated with 0.5 M trichloroacetic acid and following with neutral lipid extraction using MeOH:$CHCl_3$ (2:1) and acidic lipid extracted with MeOH:$CHCl_3$:12 M HCl (80:40:1). Lipids collected from split organic phase were dried before analysis.

FRET-based PKC activity reporter

The NucCKAR construct was developed by Gallegos and colleagues (36) and obtained from Addgene (plasmid # 14869). Cells were transfected using Fugene6 (Promega) and microscope studies performed in 48 hours. 200 nM phorbol-12,13-dibutyrate (PdBu) (Sigma-Aldrich) was used as a positive control. 250 nM Gö6983 (Tocris Bioscience, Bristol, UK) was used as a PKC inhibitor to confirm the specificity of EGF response. Pre-stimulation baseline was

performed with only DMSO before perfusion with PdBu and Gö6983 as a vehicle control. Cells were placed in a custom-made perfusion chamber for agonist stimulation. Cyan fluorescent protein (CFP) and yellow fluorescent protein (YFP) emission intensity were collected using a Zeiss LSM 710 DUO NLO with a 63X, 1.4 NA objective lens. With this construct, increased PKC activity results in decreased rather than increased FRET (36). Therefore, CFP/YFP rather than YFP/CFP emission ratio was calculated to reflect PKC activity (36), and normalized using Microsoft Excel software.

FRET-based $InsP_3$ reporter

The FRET-based $InsP_3$-biosensor with nuclear localization signal (FIRE-1nuc) was developed by Kapoor and colleagues (57). Cells were transfected using Fugene6 (Promega) and microscope studies performed in 48 hours. Cells were placed in a custom-made perfusion chamber for agonist stimulation. Cyan fluorescent protein (CFP) and yellow fluorescent protein (YFP) emission intensity were collected using a Zeiss LSM 710 DUO NLO with a 63X, 1.4 NA objective lens. YFP/CFP emission ratio was calculated and normalized using ZEN (Zeiss), Microsoft Excel and GraphPad Prism software.

Proliferation assays

SKHEP-1 cells were seeded into 96-well plates (Corning, NY, USA) at a density of $1x10^4$ and transfected with Lipofectamine RNAiMAX with control siRNAs, PLCδ4 siRNAs, and PLCγ1 siRNAs. The cells were transfected with 50 nM of each siRNA. Cells without transfection reagent and with Lipofectamine were used as a control group. The Cell Proliferation Elisa kit (ROCHE, offered by Sigma-Aldrich, CA) was used according to manufacturer instructions. Briefly, after 48 hours, cells were cultivated with BrdU (0.2 µM) for two hours in serum-free media, fixated for 30 min and incubated with anti-BrdU-POD for 90 min at room temperature. After three washing steps, TMB was added, and the plate was read at 370 and 492 nm (Synergy 2, Biotek).

For proliferation curve assay, SKHep-1 cells were transfected with control siRNA 1 or PLCδ4 siRNA 1. After 48 hours, cells were collected by trypsinization and counted in a Neubauer chamber using Trypan blue for viability exclusion, in triplicate.

For the proliferation recovery experiment, the Tet-pLKO-neo plasmid (Addgene ID. 21916) was used to express shRNAs under the control of doxycycline promoter. The PLCD4 shRNAs target sequences were obtained from "The RNAi Consortium collection" (https://portals.broadinstitute.org/gpp/public/), and the shRNA were designed and cloned according to Addgene instructions. In summary, shRNA sequences were subcloned into Tet-pLKO-neo after digestion with AgeI and EcoR1. We used the following target sequences for the shRNAs: PLCδ4 shRNA 1 (5´-AGAGCAGCGTCGAGGGATATA-3`), PLCδ4 shRNA 2 (5´-ACTACCACTTCTACGAGATAT-3`), scramble shRNA 1 (5´-CCTAAGGTTAAGT CGCCCTCG-3`) and scramble shRNA 2 (5`-CUUCCUCUCUUUCUCUCCCUUGUGA-3`). SKHep-1 cells were transfected and selected with 500 ng/mL of G418. Stable cells were treated with 1 µg/mL doxycycline for 48 hours and them were kept without doxycycline for another 48 hours for PLCδ4 expression recovery. BrDU assay was performed as described above.

Cell death assay

For this experiment, the cells were incubated with 10 µg/mL doxorubicin for 24 hours, as a positive control for cell death. The cells were incubated with Annexin V-FITC (Life Technologies) and propidium iodide (Life Technologies) for 1 hour. Images were collected with a 10X and 20X objective lens on an Olympus IX70 inverted fluorescence microscopy (Olympus America, Melville, NY), the data obtained were quantified by counting cell labeled for Annexin V-FITC, PI, double-labeled and crossed with Bright-field images were used to obtain total cell count. Each treatment was made in triplicate, three different images were counted, and the means were used for statistical analysis.

Statistical analysis

The significance of changes in treatment groups was determined by Student's t-test or one-way analysis of variance with Turkey's multiple comparison tests if not otherwise stated, using GraphPad Prism software. Data are represented as mean ± S.E.

Acknowledgments
We acknowledge Dr. Maria Ciarleglio for the statistical consultation. This work was supported by the NIH grants R03 TW08709, P01 DK57751, P30 DK34989, S10 OD023598 and R01 DK45710, DK114041 and DK112797, and by grants from the "*INCT-Regenera*", "*Rede Mineira de Engenharia de Tecidos e Terapia Celular* (REMETTEC, RED-00570-16)," FAPEMIG, CAPES, and CNPq. The authors also thank "*Centro de Aquisição e Processamento de Imagens do ICB/UFMG*" (CAPI) for technical support.

Conflict of interest
We declare that there are no conflicts of interest.

References

1. Berridge, M. J. (2016) The Inositol Trisphosphate/Calcium Signaling Pathway in Health and Disease. *Physiol. Rev.* **96**, 1261–1296
2. Pusl, T., Wu, J. J., Zimmerman, T. L., Zhang, L., Ehrlich, B. E., Berchtold, M. W., Hoek, J. B., Karpen, S. J., Nathanson, M. H., and Bennett, A. M. (2002) Epidermal growth factor-mediated activation of the ETS domain transcription factor Elk-1 requires nuclear calcium. *J. Biol. Chem.* **277**, 27517–27
3. Rodrigues, M. A., Gomes, D. A., Leite, M. F., Grant, W., Zhang, L., Lam, W., Cheng, Y.-C., Bennett, A. M., and Nathanson, M. H. (2007) Nucleoplasmic calcium is required for cell proliferation. *J. Biol. Chem.* **282**, 17061–8
4. Hardingham, G. E., Chawla, S., Johnson, C. M., and Bading, H. (1997) Distinct functions of nuclear and cytoplasmic calcium in the control of gene expression. *Nature*. **385**, 260–265
5. Echevarria, W., Leite, M. F., Guerra, M. T., Zipfel, W. R., and Nathanson, M. H. (2003) Regulation of calcium signals in the nucleus by a nucleoplasmic reticulum. *Nat Cell Biol*. **5**, 440–446
6. Gomes, D. A., Leite, M. F., Bennett, A. M., and Nathanson, M. H. (2006) Calcium signaling in the nucleus. *Can. J. Physiol. Pharmacol.* **84**, 325–332
7. Gomes, D. A., Rodrigues, M. A., Leite, M. F., Gomez, M. V, Varnai, P., Balla, T., Bennett, A. M., and Nathanson, M. H. (2008) c-Met must translocate to the nucleus to initiate calcium signals. *J. Biol. Chem.* **283**, 4344–51
8. Rodrigues, M. A., Gomes, D. A., Andrade, V. A., Leite, M. F., and Nathanson, M. H. (2008) Insulin induces calcium signals in the nucleus of rat hepatocytes. *Hepatology*. 10.1002/hep.22424
9. Subramanian, K., and Meyer, T. (1997) Calcium-induced restructuring of nuclear envelope and endoplasmic reticulum calcium stores. *Cell*. **89**, 963–71
10. Malhas, A., Goulbourne, C., and Vaux, D. J. (2011) The nucleoplasmic reticulum: form and function. *Trends Cell Biol.* **21**, 362–73
11. Stehno-Bittel, L., Lückhoff, A., and Clapham, D. E. (1995) Calcium release from the nucleus by InsP3 receptor channels. *Neuron*. **14**, 163–7
12. Khamphaya, T., Chukijrungroat, N., Saengsirisuwan, V., Mitchell-Richards, K. A., Robert, M. E., Mennone, A., Ananthanarayanan, M., Nathanson, M. H., and Weerachayaphorn, J. (2018) Nonalcoholic fatty liver disease impairs expression of the type II inositol 1,4,5-trisphosphate receptor. *Hepatology*. **67**, 560–574
13. Ueasilamongkol, P., Khamphaya, T., Guerra, M. T., Rodrigues, M. A., Gomes, D. A., Kong, Y., Wei, W., Jain, D., Trampert, D. C., Ananthanarayanan, M., Banales, J. M., Roberts, L. R., Farshidfar, F., Nathanson, M. H., and Weerachayaphorn, J. (2019) Type 3 inositol 1,4,5-trisphosphate receptor is increased and enhances malignant properties in cholangiocarcinoma. *Hepatology*. 10.1002/hep.30839
14. Brand, T. M., Iida, M., Li, C., and Wheeler, D. L. (2011) The nuclear epidermal growth factor

receptor signaling network and its role in cancer. *Discov Med*. **12**, 419–432
15. Li, C., Iida, M., Dunn, E. F., Ghia, A. J., and Wheeler, D. L. (2009) Nuclear EGFR contributes to acquired resistance to cetuximab. *Oncogene*. **28**, 3801–3813
16. Huang, W. C., Chen, Y. J., Li, L. Y., Wei, Y. L., Hsu, S. C., Tsai, S. L., Chiu, P. C., Huang, W. P., Wang, Y. N., Chen, C. H., Chang, W. C., Chang, W. C., Chen, A. J., Tsai, C. H., and Hung, M. C. (2011) Nuclear translocation of epidermal growth factor receptor by Akt-dependent phosphorylation enhances breast cancer-resistant protein expression in gefitinib-resistant cells. *J Biol Chem*. **286**, 20558–20568
17. De Angelis Campos, A. C., Rodrigues, M. A., de Andrade, C., de Goes, A. M., Nathanson, M. H., and Gomes, D. A. (2011) Epidermal growth factor receptors destined for the nucleus are internalized via a clathrin-dependent pathway. *Biochem Biophys Res Commun*. 10.1016/j.bbrc.2011.07.100
18. Faraco, C. C. F., Faria, J. A. Q. A., Kunrath-Lima, M., Miranda, M. C. D., de Melo, M. I. A., Ferreira, A. D. F., Rodrigues, M. A., and Gomes, D. A. (2017) Translocation of Epidermal Growth Factor (EGF) to the nucleus has distinct kinetics between adipose tissue-derived mesenchymal stem cells and a mesenchymal cancer cell lineage. *J. Struct. Biol.* 10.1016/j.jsb.2017.12.007
19. Lin, S. Y., Makino, K., Xia, W., Matin, a, Wen, Y., Kwong, K. Y., Bourguignon, L., and Hung, M. C. (2001) Nuclear localization of EGF receptor and its potential new role as a transcription factor. *Nat. Cell Biol.* **3**, 802–8
20. Huo, L., Wang, Y. N., Xia, W., Hsu, S. C., Lai, C. C., Li, L. Y., Chang, W. C., Wang, Y., Hsu, M. C., Yu, Y. L., Huang, T. H., Ding, Q., Chen, C. H., Tsai, C. H., and Hung, M. C. (2010) RNA helicase A is a DNA-binding partner for EGFR-mediated transcriptional activation in the nucleus. *Proc Natl Acad Sci U S A*. **107**, 16125–16130
21. Wang, S. C., Nakajima, Y., Yu, Y. L., Xia, W., Chen, C. T., Yang, C. C., McIntush, E. W., Li, L. Y., Hawke, D. H., Kobayashi, R., and Hung, M. C. (2006) Tyrosine phosphorylation controls PCNA function through protein stability. *Nat Cell Biol*. **8**, 1359–1368
22. Liccardi, G., Hartley, J. A., and Hochhauser, D. (2011) EGFR nuclear translocation modulates DNA repair following cisplatin and ionizing radiation treatment. *Cancer Res*. **71**, 1103–1114
23. Wang, Y. N., and Hung, M. C. (2012) Nuclear functions and subcellular trafficking mechanisms of the epidermal growth factor receptor family. *Cell Biosci*. **2**, 13
24. Bootman, M. D., Fearnley, C., Smyrnias, I., MacDonald, F., and Roderick, H. L. (2009) An update on nuclear calcium signalling. *J. Cell Sci.* **122**, 2337–2350
25. Nakamura, Y., and Fukami, K. (2017) Regulation and physiological functions of mammalian phospholipase C. *J. Biochem.* **161**, mvw094
26. Faenza, I., Fiume, R., Piazzi, M., Colantoni, A., and Cocco, L. (2013) Nuclear inositide specific phospholipase C signalling - Interactions and activity. *FEBS J.* **280**, 6311–6321
27. Leung, D. W., Tompkins, C., Brewer, J., Ball, A., Coon, M., Morris, V., Waggoner, D., and Singer, J. W. (2004) Phospholipase C delta-4 overexpression upregulates ErB1/2 expression, Erk signaling pathway, and proliferation in MCF-7 cells. *Mol. Cancer*. 10.1186/1476-4598-3-15
28. Ratti, S., Mongiorgi, S., Ramazzotti, G., Follo, M. Y., Mariani, G. A., Suh, P. G., McCubrey, J. A., Cocco, L., and Manzoli, L. (2017) Nuclear Inositide Signaling Via Phospholipase C. *J. Cell. Biochem.* **118**, 1969–1978
29. Lee, S. B., and Rhee, S. G. (1996) Molecular cloning, splice variants, expression, and purification of phospholipase C-delta 4. *J. Biol. Chem.* **271**, 25–31
30. Nagano, K., Fukami, K., Minagawa, T., Watanabe, Y., Ozaki, C., and Takenawa, T. (1999) A novel phospholipase C delta4 (PLCdelta4) splice variant as a negative regulator of PLC. *J. Biol. Chem.* **274**, 2872–9
31. Kunrath-Lima, M., de Miranda, M. C., Ferreira, A. da F., Faraco, C. C. F., de Melo, M. I. A., Goes, A. M., Rodrigues, M. A., Faria, J. A. Q. A., and Gomes, D. A. (2018) Phospholipase C delta 4 (PLCδ4) is a nuclear protein involved in cell proliferation and senescence in mesenchymal stromal stem cells. *Cell. Signal.* **49**, 59–67

32. Asano, M., Tamiya-Koizumi, K., Homma, Y., Takenawa, T., Nimura, Y., Kojima, K., and Yoshida, S. (1994) Purification and characterization of nuclear phospholipase C specific for phosphoinositides. *J. Biol. Chem.* **269**, 12360–12366
33. Liu, N., Fukami, K., Yu, H., and Takenawa, T. (1996) A new phospholipase C delta 4 is induced at S-phase of the cell cycle and appears in the nucleus. *J Biol Chem*. **271**, 355–360
34. Moccia, F., Berra-Romani, R., Tritto, S., Signorelli, S., Taglietti, V., and Tanzi, F. (2003) Epidermal growth factor induces intracellular Ca2+ oscillations in microvascular endothelial cells. *J Cell Physiol*. **194**, 139–150
35. Martelli, A. M., Evangelisti, C., Nyakern, M., and Manzoli, F. A. (2006) Nuclear protein kinase C. *Biochim Biophys Acta*. **1761**, 542–551
36. Gallegos, L. L., Kunkel, M. T., and Newton, A. C. (2006) Targeting protein kinase C activity reporter to discrete intracellular regions reveals spatiotemporal differences in agonist-dependent signaling. *J Biol Chem*. **281**, 30947–30956
37. Shi, Y., Tao, Y., Jiang, Y., Xu, Y., Yan, B., Chen, X., Xiao, L., and Cao, Y. (2012) Nuclear epidermal growth factor receptor interacts with transcriptional intermediary factor 2 to activate cyclin D1 gene expression triggered by the oncoprotein latent membrane protein 1. *Carcinogenesis*. **33**, 1468–1478
38. Sandvig, K., and Van Deurs, B. (2002) Transport of protein toxins into cells: Pathways used by ricin, cholera toxin and Shiga toxin. *FEBS Lett.* **529**, 49–53
39. Marsh, M., and Helenius, A. (2006) Virus entry: Open sesame. *Cell*. **124**, 729–740
40. Carpenter, G., and Liao, H. J. (2009) Trafficking of receptor tyrosine kinases to the nucleus. *Exp. Cell Res.* **315**, 1556–1566
41. Follo, M. Y., Finelli, C., Mongiorgi, S., Clissa, C., Bosi, C., Testoni, N., Chiarini, F., Ramazzotti, G., Baccarani, M., Martelli, A. M., Manzoli, L., Martinelli, G., and Cocco, L. (2009) Reduction of phosphoinositide-phospholipase C beta1 methylation predicts the responsiveness to azacitidine in high-risk MDS. *Proc Natl Acad Sci U S A*. **106**, 16811–16816
42. Nishibe, S., Wahl, M. I., Hernández-Sotomayor, S. M., Tonks, N. K., Rhee, S. G., and Carpenter, G. (1990) Increase of the catalytic activity of phospholipase C-gamma 1 by tyrosine phosphorylation. *Science*. **250**, 1253–6
43. Kumar, V., Jong, Y. J., and O'Malley, K. L. (2008) Activated nuclear metabotropic glutamate receptor mGlu5 couples to nuclear Gq/11 proteins to generate inositol 1,4,5-trisphosphate-mediated nuclear Ca2+ release. *J Biol Chem*. **283**, 14072–14083
44. Manzoli, L., Billi, A. M., Rubbini, S., Bavelloni, A., Faenza, I., Gilmour, R. S., Rhee, S. G., and Cocco, L. (1997) Essential role for nuclear phospholipase C beta1 in insulin-like growth factor I-induced mitogenesis. *Cancer Res*. **57**, 2137–2139
45. Faenza, I., Ramazzotti, G., Bavelloni, A., Fiume, R., Gaboardi, G. C., Follo, M. Y., Gilmour, R. S., Martelli, A. M., Ravid, K., and Cocco, L. (2007) Inositide-dependent phospholipase C signaling mimics insulin in skeletal muscle differentiation by affecting specific regions of the cyclin D3 promoter. *Endocrinology*. **148**, 1108–1117
46. Ramazzotti, G., Faenza, I., Gaboardi, G. C., Piazzi, M., Bavelloni, A., Fiume, R., Manzoli, L., Martelli, A. M., and Cocco, L. (2008) Catalytic activity of nuclear PLC-beta(1) is required for its signalling function during C2C12 differentiation. *Cell Signal*. **20**, 2013–2021
47. Huang, W., Mishra, V., Batra, S., Dillon, I., and Mehta, K. D. (2004) Phorbol ester promotes histone H3-Ser10 phosphorylation at the LDL receptor promoter in a protein kinase C-dependent manner. *J Lipid Res*. **45**, 1519–1527
48. Parekh, D. B., Ziegler, W., and Parker, P. J. (2000) Multiple pathways control protein kinase C phosphorylation. *EMBO J*. **19**, 496–503
49. Fima, E., Shtutman, M., Libros, P., Missel, A., Shahaf, G., Kahana, G., and Livneh, E. (2001) PKCeta enhances cell cycle progression, the expression of G1 cyclins and p21 in MCF-7 cells. *Oncogene*. **20**, 6794–6804
50. Poli, A., Faenza, I., Chiarini, F., Matteucci, A., McCubrey, J. A., and Cocco, L. (2013) K562 cell

proliferation is modulated by PLCbeta1 through a PKCalpha-mediated pathway. *Cell Cycle*. **12**, 1713–1721
51. Poli, A., Ramazzotti, G., Matteucci, A., Manzoli, L., Lonetti, A., Suh, P. G., McCubrey, J. A., and Cocco, L. (2014) A novel DAG-dependent mechanism links PKCa and Cyclin B1 regulating cell cycle progression. *Oncotarget*. **5**, 11526–11540
52. Fiume, R., Ramazzotti, G., Teti, G., Chiarini, F., Faenza, I., Mazzotti, G., Billi, A. M., and Cocco, L. (2009) Involvement of nuclear PLCbeta1 in lamin B1 phosphorylation and G2/M cell cycle progression. *FASEB J*. **23**, 957–966
53. Michalopoulos, G. K. (2017) Hepatostat: Liver regeneration and normal liver tissue maintenance. *Hepatology*. **65**, 1384–1392
54. Liu, N., Fukami, K., Yu, H., and Takenawa, T. (1996) A new phospholipase C delta 4 is induced at S-phase of the cell cycle and appears in the nucleus. *J. Biol. Chem.* **271**, 355–60
55. Akutagawa, A., Fukami, K., Banno, Y., Takenawa, T., Kannagi, R., Yokoyama, Y., Oda, K., Nagino, M., Nimura, Y., Yoshida, S., and Tamiya-Koizumi, K. (2006) Disruption of phospholipase Cdelta4 gene modulates the liver regeneration in cooperation with nuclear protein kinase C. *J Biochem*. **140**, 619–625
56. Boyer, J. L., Phillips, J. M., and Graf, J. (1990) Preparation and specific applications of isolated hepatocyte couplets. *Methods Enzym.* **192**, 501–516
57. Kapoor, N., Maxwell, J. T., Mignery, G. A., Will, D., Blatter, L. A., and Banach, K. (2014) Spatially Defined InsP3-Mediated Signaling in Embryonic Stem Cell-Derived Cardiomyocytes. *PLoS One*. **9**, e83715

Abbreviations:

AVP, arginine vasopressin; CHC2, Clathrin heavy chain 2; CFP, cyan fluorescent protein; DAG, diacylglycerol; EGF, epidermal growth factor; EGFR, EGF receptor; ER, endoplasmic reticulum; FRET, förster resonance energy transfer; $InsP_3$, inositol 1,4,5-trisphosphate; $InsP_3R$, $InsP_3$ Receptor; mRFP, monomeric red fluorescent protein; NE, nuclear envelope; NR, nucleoplasmic reticulum; PdBu, phorbol 12-13-dibutyrate; $PI(4,5)P_2$, phosphatidylinositol 4,5-bisphosphate; PKC, protein kinase C; PLC, phospholipase C; RTK, receptor tyrosine kinase; YFP, yellow fluorescent protein.

Figure legends

Figure 1: EGF induces EGFR nuclear translocation and Clathrin-mediated endocytosis-dependent Ca^{2+} signals. **A**, Western blot analysis of EGFR in non-nuclear and nuclear fractions isolated from resting (control) or EGF-stimulated hepatocyte and SKHep-1 cells. α-Tubulin and Lamin B1 were used as purity controls for non-nuclear and nuclear fractions, respectively. Indicated kDa values represent the position of the referenced bands from pre-stained protein standard. Densitometric measurements of cellular fractions show that nuclear EGFR is maximal within 10 min of stimulation in SKHep-1 cells and within 2.5-5 min ($p<0.01$) in hepatocytes when compared with the control (0 min). Values are scaled relative to the initial amount in the non-nuclear fraction and relative to the amount at 2.5 min in the nuclear fraction (mean ± S.E.; n = 3) (Nuclear SKHep-1 fractions - One-Way ANOVA, $F(4,10)=3.215$; $p=0.0611$; Nuclear Hepatocyte fractions - One-Way ANOVA, $F(4,10)=8.530$, $p=0.0029$). **B**, Gated STED super-resolution images of control SKHep-1 cells (right image) and 10 min after EGF stimulation (middle image). Serial optical sections were collected for three-dimensional reconstruction; y-z sections are shown at the right of each image. EGFR is represented in green, Lamin B1 is in red and the nuclear compartment marked in blue. Note that EGFR redistributes to the region of the nuclear envelope as well as in within the nuclear interior (arrows). Bar = 10 micrometers. Scatter plot (right panel) showing the quantification of EGFR that co-localizes with the nucleus before and after EGF stimulation. N = 7-12 cells for each group. The image collection settings for fluorescence quantification was adjusted according to the cells stimulated with EGF to avoid nuclear-saturated pixels of EGFR clusters. ***$p<0.001$ (Student's t-test). **C**, western blot (top) analysis of clathrin heavy chain 2 (CHC2) expression in non-treated, lipofectamine only, control siRNAs-treated or CHC2 siRNAs-treated SKHep-1 cells. α-Tubulin was used as a loading control. Bar graph showing the summary of the western blots (n=4), ***$p<0.001$. (One-Way ANOVA, $F(5,18)=34.41$; $P<0.0001$). **D**, Tracings represent Fluo-4/AM fluorescence intensity changes, normalized by the baseline, by the time of EGF stimulation. Lower panel, bar graph compiling peaks of Fluo-4/AM fluorescence intensity in EGF-stimulated at 15 min, control siRNA-treated (n=15), lipofectamine only (n=14), control siRNA 1 (n=10), control siRNA 2 (n=10), CHC2 siRNA 1 (n=13) or CHC2 siRNA 2-treated (n=13) SKHep-1 cells. Fluorescence changes over time from whole cells were normalized and represented as fluorescence intensity (F) by baseline fluorescence (F_0) multiplied by 100. ***$p<0.001$. (One-Way ANOVA, $F(5,69)=18.78$; $p<0.0001$). Experiments were performed on at least 3 different days.

Figure 2: EGF triggers Ca^{2+} release by nuclear $InsP_3$ and nuclear $PI(4,5)P_2$ hydrolysis. **A**, confocal images of SKHep-1 cells loaded with Fluo-4/AM expressing cytosolic $InsP_3$-buffer, nuclear $InsP_3$-buffer or mRFP (control). Images show cells before EGF stimulus (baseline) and the peak (15 min) of EGF-

induced Fluo-4/AM fluorescence intensity changes. Expression of constructs was checked by detection of mRFP. Bar = 10 micrometers. **B**, bar graph showing Fluo-4/AM fluorescence intensity peak in cytosolic and nuclear regions of control, cytosolic or nuclear $InsP_3$-buffer expressing cells upon EGF stimulus (8 to 11 cells in each group, *p<0.05, **p<0.01, ***p<0.001) (Cytosol – One-Way ANOVA, F(2,24)=17.17; p<0.0001; Nuclear – One-Way ANOVA, F(2,26)=28.03; p<0.0001). **C**, average traces of SKHep-1 expressing cytosolic or nuclear $InsP_3$-buffer, or control cells stimulated with EGF. Cytosolic or nuclear regions for fluorescent intensity measurements were selected using the assistance of the Digital Image of Contrast (D.I.C) images, see squares at the nucleus and non-nuclear regions. Nuclear but not cytosolic $InsP_3$-buffer blocked the peak of EGF response in both compartments. **D**, bar graph represents the amount of $PI(4,5)P_2$ of nucleus isolated from control or EGF-stimulated hepatocytes (n=6). 5 min of EGF stimulation reduces nuclear $PI(4,5)P_2$ by 64 ± 1.5% (p<0.05) (Student's t-test).

Figure 3: EGF induces nuclear PKC activity. **A**, confocal images of a representative SKHep-1 cell expressing NucCKAR shows CFP and YFP emission as well as a transmitted image of the cell, confirming nuclear localization of the construct. Bar = 10 micrometers. **B**, representative tracings of NucCKAR CFP/YFP emission normalized by baseline, shows changes in emission ratio during 30 min of perfusion with 200 nM of phorbol 12-13-dibutyrate (PdBu) (n=6), 100 ng/mL of EGF (n=10) or 500 nM of arginine vasopressin (AVP) (n=3). **C**, bar graph compiling the average results showed in B. NucCKAR FRET ratio change in EGF-stimulated cells in the presence (n=8) or absence (n=10) of the PKC inhibitor Go6983 (250 nM). The PKC inhibitor significantly attenuates EGF-induced NucCKAR FRET changes, *p<0.05 (One-Way ANOVA, F(3,23)=5.645; p=0.0002).

Figure 4: PLCγ1 is a cytosolic and PLCδ4 is a nuclear protein. **A**, representative confocal images of SKHep-1 cells before and after EGF stimulation showing PLCγ1 in red, EGFR in green and TO-PRO nuclear dye in blue. Merged images reveal that PLCγ1 is predominantly expressed outside of the nucleus in both conditions (n=15 cells). **B**, representative confocal images of control and EGF-stimulated SKHep-1 cells showing PLCδ4 in red, which is exclusively intra-nuclear (n=15 cells). **C**, Western blot showing PLCγ1 and PLCδ4 expressions in non-nuclear and nuclear fractions from control or EGF-stimulated hepatocytes. α-Tubulin and Lamin B1 were used as purity controls for nuclear and non-nuclear fractions. Indicated kDa values represent the position of the reference bands from pre-stained protein standard. Subcellular localization of PLCγ1 and PLCδ4 in hepatocytes are not altered by EGF stimulation for 10 min (n=3). **D**, tracings of normalized amounts of PLCγ1 in non-nuclear and nuclear fractions of SKHep-1 cells upon EGF stimulation with different time points, quantified from western blot experiments (n=3).

Figure 5: Intra-nuclear PLCδ4 mediates EGF-induced nuclear PI(4,5)P_2 depletion and Ca^{2+} signals. **A**, western blot showing PLCγ1 and PLCδ4 expression in SKHep-1 cells under control, lipofectamine, control siRNAs, siRNAs for PLCδ4 or PLCγ1 siRNAs-treated conditions. α-Tubulin was used as a loading control. The molecular weight of each protein analyzed is on the right side. Bar graphs showing the summary of the western blots. Specific siRNAs reduced PLCγ1 expression by 90 ± 14% and 91 ± 27% using siRNA 1 and 2, respectively (One-Way ANOVA, $F(7,16)=26.60$; $p<0.001$). PLCδ4 expressions were reduced by 75 ± 7% and 86 ± 5% using siRNA 1 and 2, respectively (**$p<0.01$) (One-Way ANOVA, $F(7,32)=5.808$; $p=0.0002$). PLCγ1 siRNAs do not alter each PLCδ4 expression levels or PLCδ4 siRNAs do not alter each PLCγ1 expression levels. **B**, graph show PI(4,5)P_2 quantification in nuclei isolated from SKHep-1 cells before (-EGF group) and after 10 min of stimulation with EGF (+EGF groups). EGF induced PI(4,5)P_2 hydrolysis was blocked by PLCδ4 siRNAs, but not by PLCγ1 siRNAs, compared to cells not treated with EGF (-EGF). Observe that -EGF group has no difference with PLCδ4 siRNAs-treated cells or PLCγ1 has no difference with EGF-treated cells. N = 3. **$p<0.01$ (One-Way ANOVA $F(8,18)=88.26$; $p<0.0001$). **C**, Left: representative average tracings of nuclear $InsP_3$ sensor (FIRE-1nuc) shows changes in YFP/CFP emission normalized by baseline in EGF-stimulated groups over 20 min. Smoothing filter was used to better discern the tracings. Right: bar graph compiling the average results shows peak intensity in control (n=11), control siRNA 1 (n=13), control siRNA 2 (n=13), PLCδ4 siRNA 1 (n=11), PLCδ4 siRNA 2 (n=12), PLCγ1 siRNA 1 (n=11) or PLCγ1 siRNA 2-treated (n=11) SKHep-1 cells. $InsP_3$ production is significantly reduced by PLCδ4 siRNAs (100 ± 0.5% for both siRNAs, *$p<0.05$), but not by PLCγ1 siRNAs, compared to control groups (One-Way ANOVA, $F(7,93)=6.717$; $p<0.0001$). **D**, Left: representative average tracings of NucCKAR CFP/YFP emission normalized by baseline, shows changes in emission ratio during 25 min of perfusion with EGF. Smoothing filter was used to better discern the tracings. Right: bar graph compiling the average results shows peak intensity in control (n=12), control siRNA 1 (n=11), control siRNA 2 (n=9), PLCδ4 siRNA 1 (n=7), PLCδ4 siRNA 2-treated (n=7), PLCγ1 siRNA 1 (n=6) or PLCγ1 siRNA 2-treated (n=8) SKHep-1 cells. PKC activation is significantly reduced by PLCδ4 siRNAs (100.7 ± 0.4% for siRNA 1 and 100 ± 0.7% for siRNA 2, *$p<0.05$), but not by PLCγ1 siRNAs, compared to control groups (Kruskal-Wallis, $H=37.85$, $df=7$, $p<0,0001$; Dunn's multiple comparisons test). **E**, Left: Average tracings represent Fluo-4/AM fluorescence intensity changes in response to EGF stimulation. Fluorescence changes over time from whole cells were normalized and are represented as fluorescence intensity (F) divided by baseline fluorescence (F_0), multiplied by 100%. Right: bar graph compiling the average results shows peak intensity in control (n=20), Lipofectamine (n=21), control siRNA 1 (n=13), control siRNA 2 (n=10), PLCδ4 siRNA 1 (n=13), PLCδ4 siRNA 2-treated (n=10), PLCγ1 siRNA 1 (n=5) or PLCγ1 siRNA 2-treated (n=9) SKHep-1 cells. Ca^{2+} is significantly reduced by PLCδ4 siRNAs (95.9 ± 2.5% for siRNA 1

and 96.9 ± 2.6% for siRNA 2, *p<0.05), but not by PLCγ1 siRNAs, compared to control groups (One-Way ANOVA, F(7,92)=15.66; p<0.0001).

Figure 6: Knockdown of PLCδ4 diminishes cell growth and decreases cyclins A and B1 without affecting cell death. A, effects of PLCδ4 depletion on cell proliferation. BrdU measurements were performed 48 hours after transfection. *p<0.05 (EGF- One-Way ANOVA, F(5,35)=8.042; p<0.0001; EGF+ One-Way ANOVA, F(5.35)=9.570; p<0.0001). **B**, quantification of cells labeled with Annexin V-FITC and propidium iodide. The bar graph shows the percentages of cells labeled with either Annexin V-FITC or propidium iodide, or double-labeled with Annexin V-FITC plus propidium iodide compared to all cells form each field. Each treatment was made in triplicate, and for each one, three different images were counted using ImageJ software, then the means were used for statistical analysis. All groups were compared to control groups (control, Lipofectamine and control siRNAs). Doxorubicin (Dox) 10 µg/mL was used as positive control and it differs from all experimental groups. ***p<0.001. Annexin V staining did not reveal differences in the level of cell death between control and siRNA-treated groups (One-Way ANOVA, F(6,71)=20.64; p<0.0001). **C**, western blot showing cyclins A and B1 expression in SKHep-1 cells under controls or siRNA-treated conditions. α-Tubulin was used as a loading control. Representative image of 3 independent experiments. Middle and right graphs, quantification of the western blots of cyclins that were normalized with the expression of α-Tubulin (n =3). *p<0.05 and ***p<0.001 (Cyclin A – One-Way ANOVA, F(6,14)=17.92; p<0.0001; Cyclin B1 – One-Way ANOVA, F(5,12)=69.17; p<0.0001). **D**, western blot showing the effects of nuclear $InsP_3$ buffer on the expression of the cyclins A and B1. Right graph, quantification of the western blots of cyclins that were normalized with the expression of α-Tubulin (n =3). **p<0.01 (Cyclin A and B1 used a Student's t-test).

Figure 7: Proposed model – EGF triggers nuclear PI(4,5)P_2 hydrolysis, local $InsP_3$ production, and Ca^{2+} release into the nucleoplasm through intra-nuclear PLCδ4, which mediates cell proliferation. Scheme of the proposed EGF-induced nuclear Ca^{2+} signaling pathway: Upon EGF binding EGFR is activated and initiates signal transducer cascades. EGFR is shuttled to the nucleus to induce downstream targets. PLCδ4 is a nuclear enzyme induced by EGF stimulus and leads to phosphatidylinositol 4,5-bisphosphate (PI(4,5)P_2) hydrolysis which generates inositol trisphosphate ($InsP_3$) and diacylglycerol (DAG). $InsP_3$ binds to $InsP_3$ receptors ($InsP_3R$) present on the inner nuclear envelope triggering Ca^{2+} release in the nucleoplasm. DAG can activate nuclear-resident PKCs. Ca^{2+} and PKCs can activate downstream targets which ultimately result in cell proliferation.

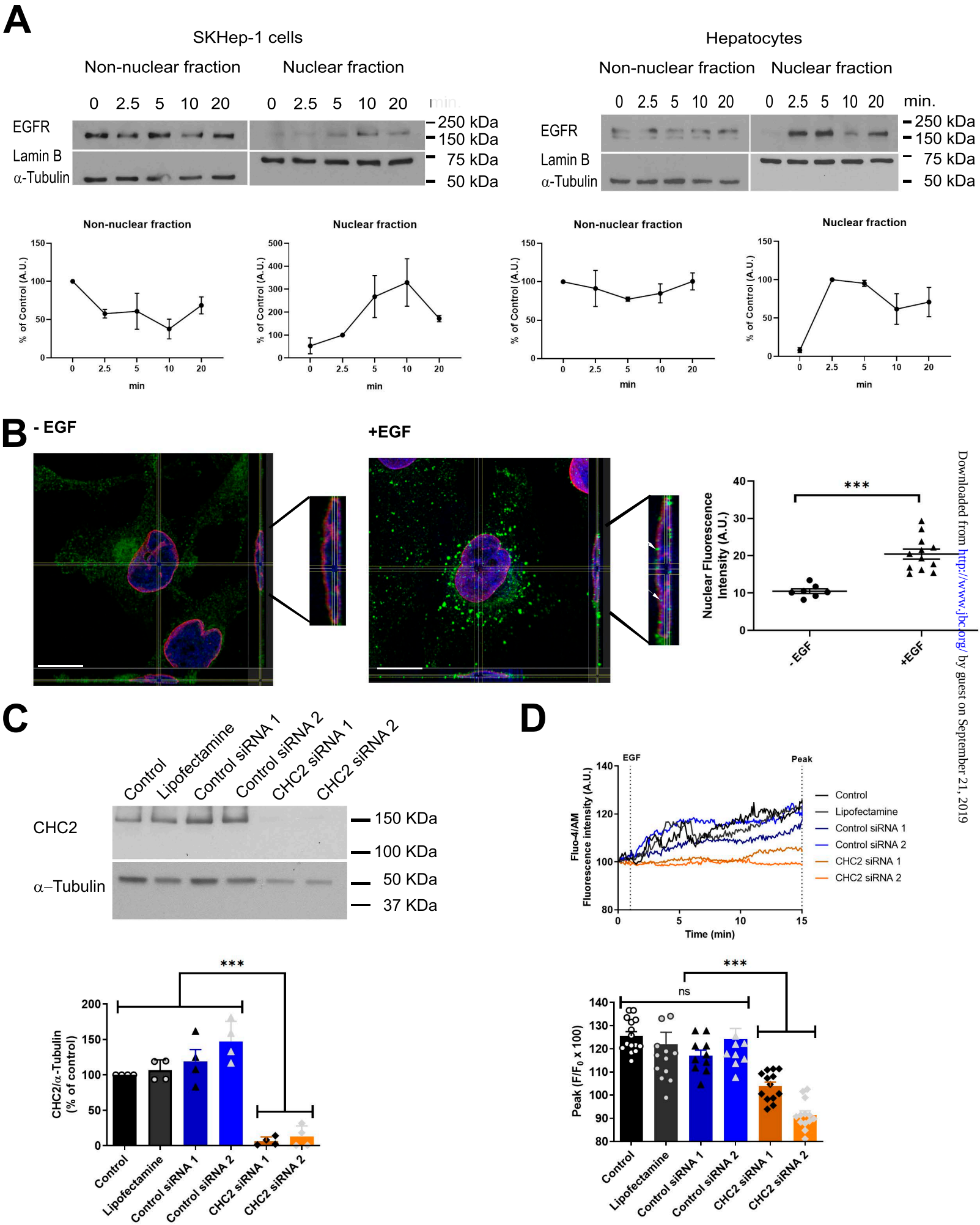

Figure 1

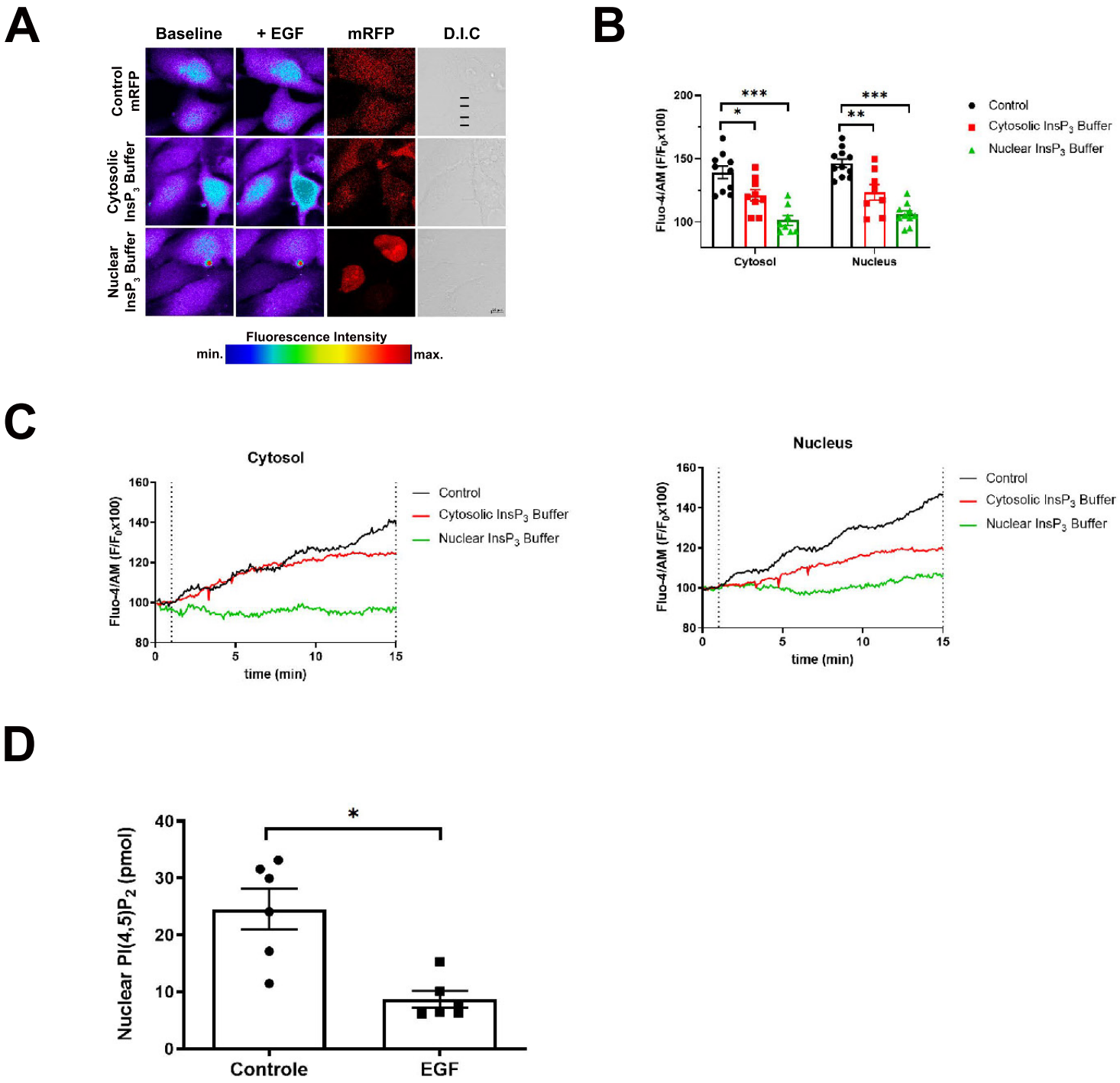

Figure 2

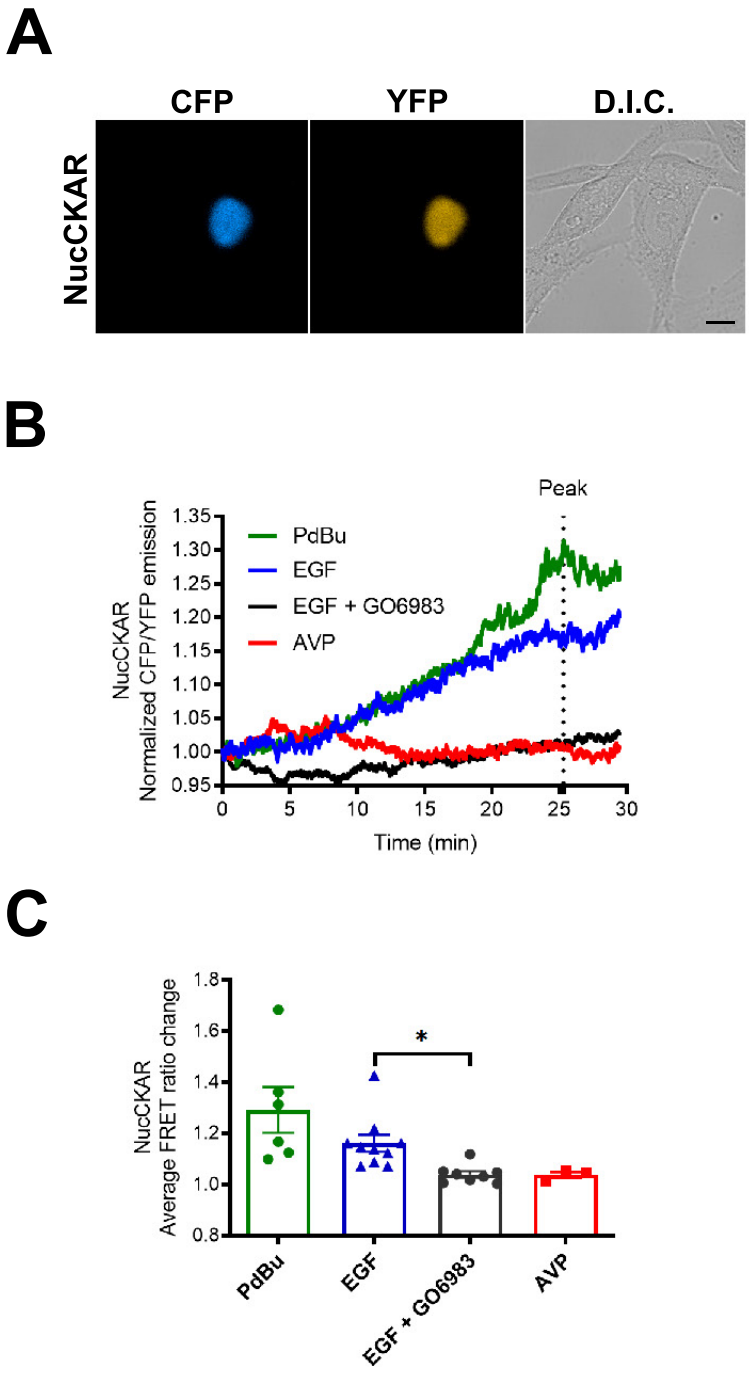

Figure 3

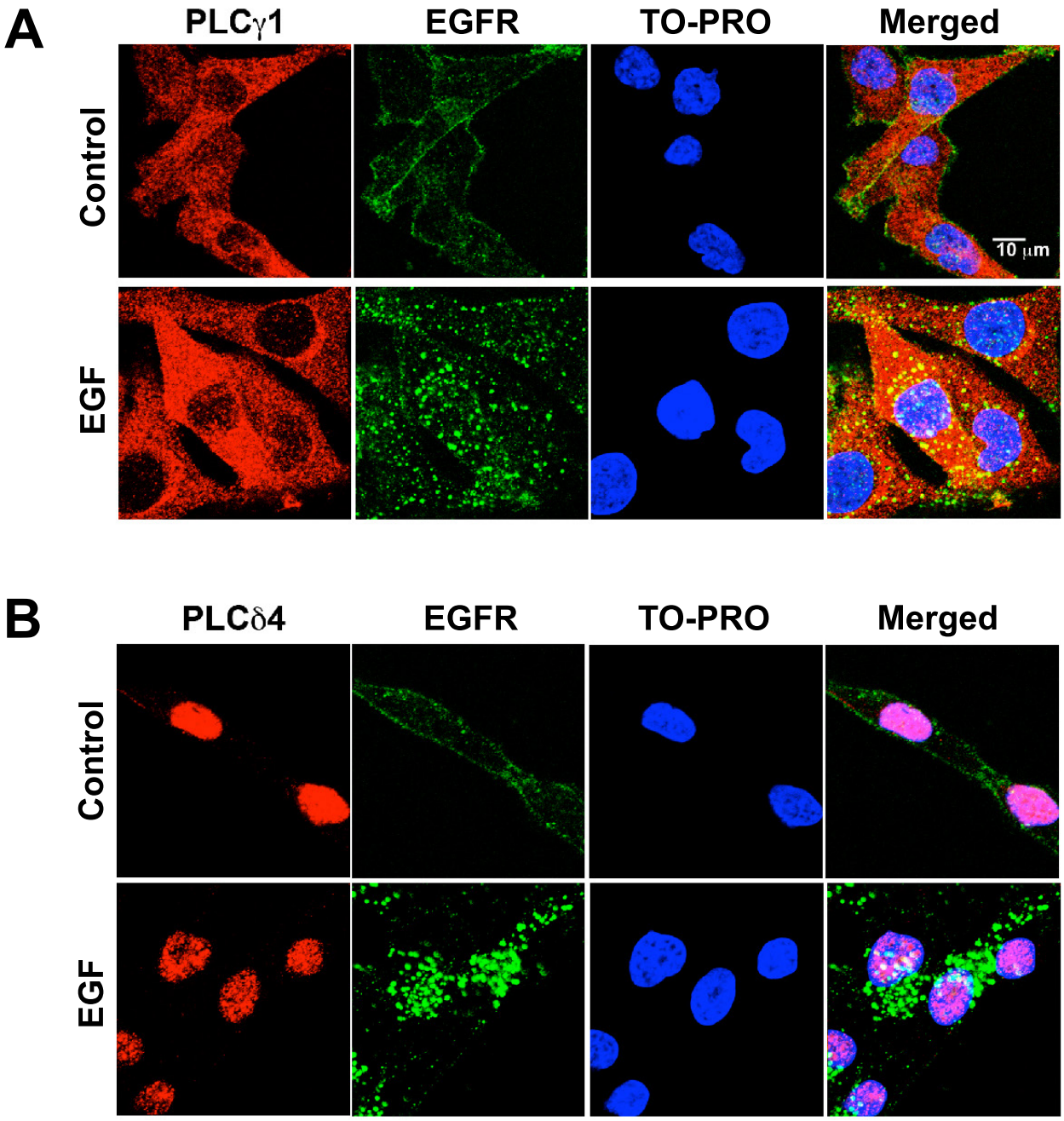

Figure 4

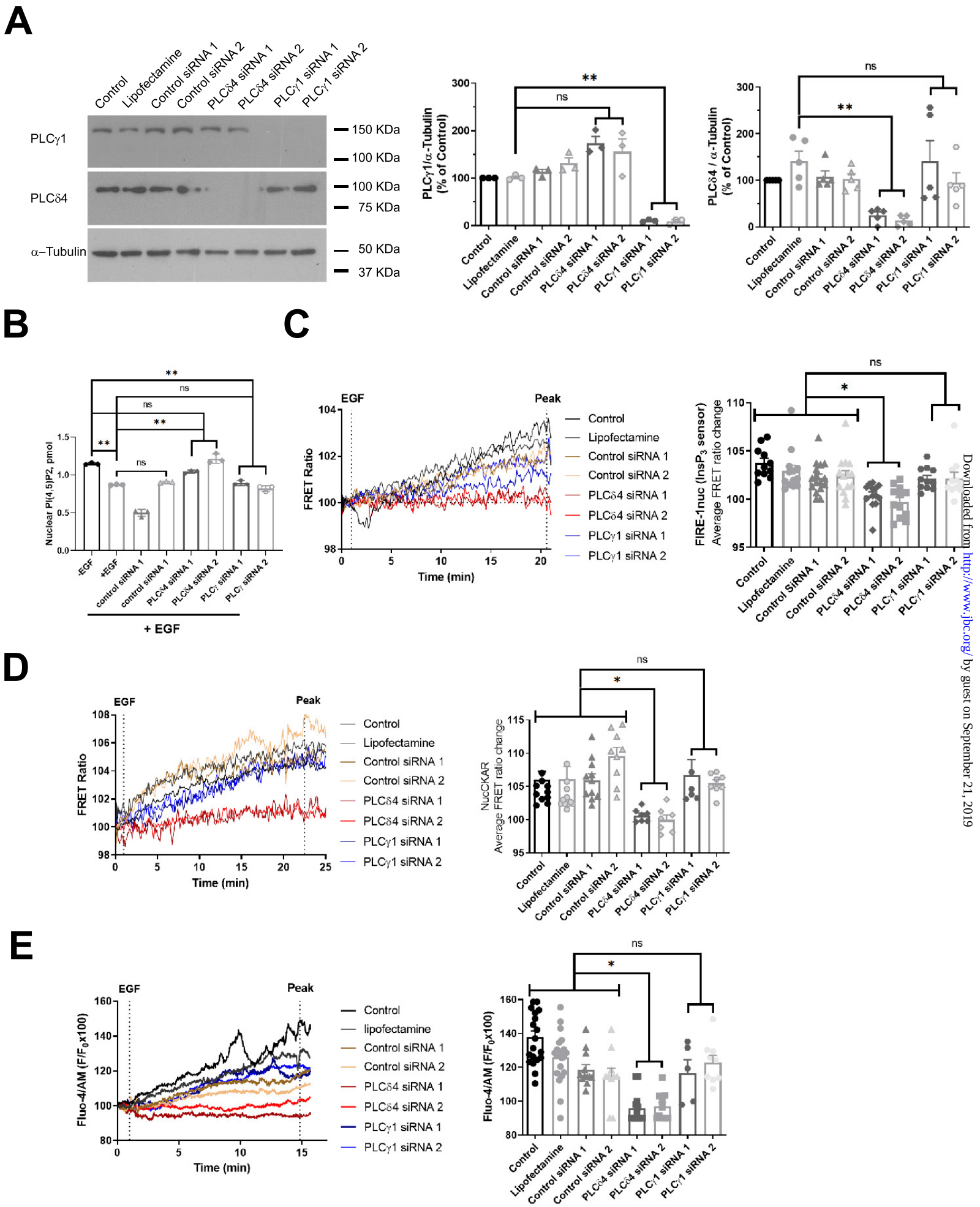

Figure 5

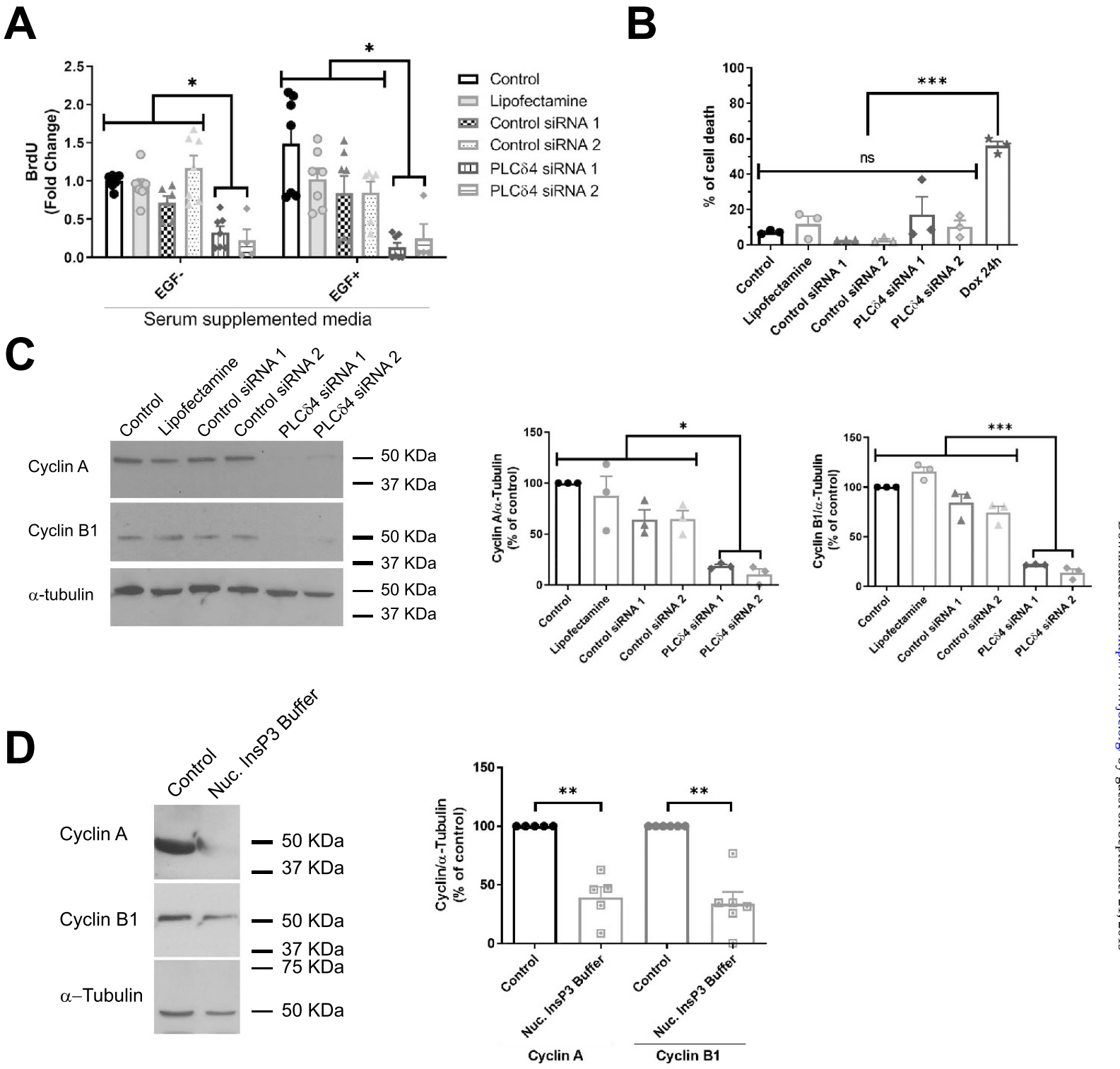

Figure 6

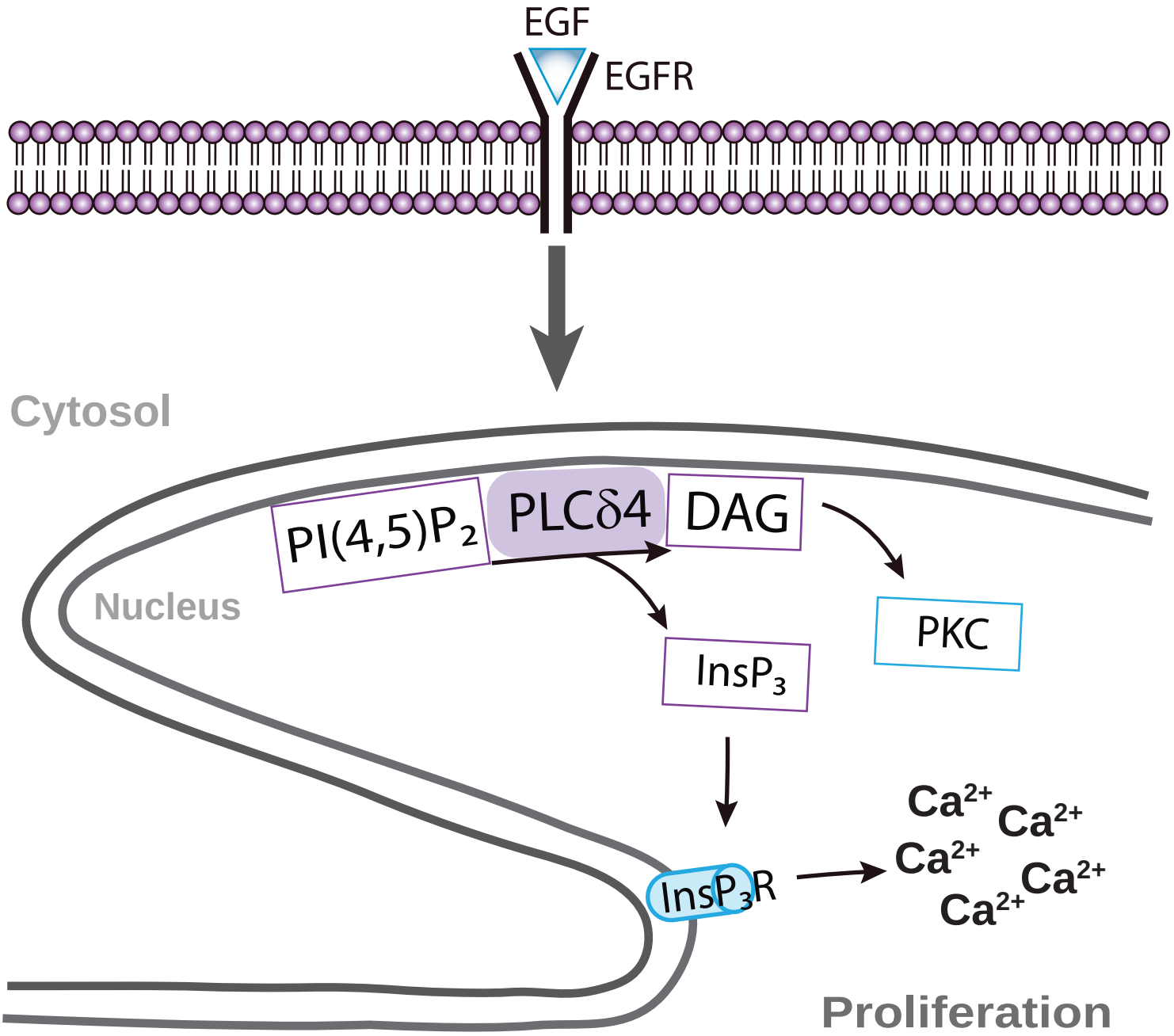

Figure 7

Epidermal growth factor (EGF) triggers nuclear calcium signaling through the intranuclear phospholipase C delta-4 (PLC δ4)

Marcelo Coutinho de Miranda, Michele Angela Rodrigues, Ana Carolina de Angelis Campos, Jerusa Araujo Quintao Arantes Faria, Marianna Kunrath-Lima, Gregory A. Mignery, Deborah Schechtman, Alfredo Miranda Goes, Michael H. Nathanson and Dawidson A. Gomes

J. Biol. Chem. published online September 19, 2019
